



The receptor protein-tyrosine phosphatase, Dep1, acts in arterial/venous cell fate decisions in zebrafish development

Fiona Rodriguez, Andrei Vacaru, John Overvoorde, Jeroen den Hertog*

Hubrecht Institute-KNAW and University Medical Center Utrecht, Uppsalaalaan 8, 3584 CT Utrecht, The Netherlands

ARTICLE INFO

Article history:

Received for publication 3 August 2007

Revised 8 September 2008

Accepted 9 September 2008

Available online 23 September 2008

Keywords:

Dep1
Protein-tyrosine phosphatase
Arterial
Venous
Cell specification
Zebrafish
Morpholino

ABSTRACT

Dep1 is a transmembrane protein-tyrosine phosphatase (PTP) that is expressed in vascular endothelial cells and has tumor suppressor activity. Mouse models with gene targeted Dep1 either show vascular defects, or do not show any defects at all. We used the zebrafish to investigate the role of Dep1 in early development. The zebrafish genome encodes two highly homologous Dep1 genes, Dep1a and Dep1b. Morpholinos specific for Dep1a and Dep1b induced defects in vasculature, resulting in defective blood circulation. However, Green Fluorescent Protein expression in *fli1a::gfp1* transgenic embryos and *cdh5* expression, markers of vascular endothelial cells, were normal upon Dep1a- and Dep1b-MO injection. Molecular markers indicated that arterial specification was reduced and venous markers were expanded in Dep1 morphants. Moreover, the Dep1a/Dep1b knockdowns were rescued by inhibition of Phosphatidylinositol-3 kinase (PI3K) and by expression of active Notch and Grl/Hey2. Our results suggest a model in which Dep1 acts upstream in a signaling pathway inhibiting PI3K, resulting in expression of Notch and Grl, thus regulating arterial specification in development.

© 2008 Elsevier Inc. All rights reserved.

Introduction

Protein phosphorylation on tyrosine residues is an important cell signaling mechanism that controls fundamental cellular processes, including proliferation, differentiation and migration. The phosphorylation state is governed by the opposing activities of protein-tyrosine kinases (PTKs) and protein-tyrosine phosphatases (PTPs) (Hunter, 1995). Like the PTKs, the PTPs represent a large family of enzymes with cytoplasmic and transmembrane members. Still relatively little is known about the function of PTPs in development.

The classical PTPs are subdivided into 17 subfamilies based on the alignment of the highly conserved catalytic PTP domain. The transmembrane PTPs are tentatively called receptor PTPs (RPTPs) because of their potential to signal across the membrane. Most RPTPs encode two cytoplasmic PTP domains. However, the R3 Receptor Protein-Tyrosine Phosphatase (RPTP) subfamily, comprising Dep1 (also known as CD148 and RPTPeta), SAP-1, PTP β and Glepp1 encode a single PTP domain (den Hertog, 1999; Alonso et al., 2004; Andersen et al., 2004). Dep1 has eight Fibronectin type III (FNIII) motifs in its extracellular region. Dep1 expression was enhanced 10-fold in WI-38 human embryonic lung fibroblasts growing in monolayer when they approached confluence, hence the name density-enhanced PTP1, Dep1 (Ostman et al., 1994).

Dep1 is expressed in vascular endothelial cells of the arterial and capillary vessels of a number of organs (Borges et al., 1996; Takahashi et al., 1999, 2003). In addition, Dep1 is expressed in different

hematopoietic derived cell lineages (de la Fuente-Garcia et al., 1998). Dep1 shows tumor suppressor activity when overexpressed in cultured tumor cells (Keane et al., 1996; Trapasso et al., 2000). The mouse *Ptprj* gene, encoding Dep1, is a candidate for the colon-cancer susceptibility locus *Sccl*. Moreover, the human *PTPRJ* gene is frequently deleted in human cancers (Ruivenkamp et al., 2002). Taken together, Dep1 is an important tumor suppressor gene.

Gene targeting of Dep1 in the mouse by in-frame replacement of cytoplasmic sequences with enhanced Green Fluorescent Protein (GFP) sequences resulted in embryos that died at midgestation, before embryonic day 11.5 with vascularization failure and disorganized vascular structures. Homozygous mutant embryos displayed subtle defects, such as enlarged vessels comprised of endothelial cells as early as embryonic day 8.25. These Dep1 mutant mice implicated a role for Dep1 in endothelial proliferation and in vascular organization during development (Takahashi et al., 2003). However, the molecular mechanisms underlying the phenotype are still unclear. Surprisingly, genetic ablation of Dep1 by deletion of exons 3, 4 and 5 by homologous recombination, did not affect mouse development. In fact, homozygous *Ptprj*^{-/-} mice are viable and fertile. Immunoblotting confirmed that these mice do not express Dep1 protein (Trapasso et al., 2006). Recent work in *C. elegans* indicated a role for Dep1 in binary cell fate decisions. Dep1 acts as a negative regulator of EGFR signaling and through an intricate feedback mechanism, Dep1 amplifies the small difference in EGFR signaling, resulting in full activation of the EGFR/RAS/MAPK pathway in primary vulval cells and inactivation of this pathway in secondary cells (Berset et al., 2005), thus effectively determining cell fate in vulval development.

* Corresponding author. Fax: +31 30 2516464.

E-mail address: j.denhertog@niob.knaw.nl (J. den Hertog).

Here, we used zebrafish to investigate the role of Dep1 in vertebrate development. The zebrafish genome encodes two Dep1 proteins, Dep1a and Dep1b. Morpholino-injections targeting Dep1a, Dep1b, or both, indicated that the two Dep1s were essential for normal blood circulation. Dep1 knockdown resulted in reduced arterial markers and expanded venous markers. Rescue experiments indicated that Phosphatidylinositol-3-Kinase (PI-3 Kinase), Grl/hey2 and Notch signaling were involved in Dep1 function. Our results indicate that Dep1 is required for the arterial-venous cell fate decision.

Results

Zebrafish dep1a and dep1b are ubiquitously expressed

The zebrafish genome encodes two *dep1* genes, *dep1a* (Zv6, ENSDARG00000011567) and *dep1b* (Zv6, ENSDARG00000033042). Zebrafish Dep1a comprises 12 Fibronectin type III like repeats, four more than mammalian Dep1. The 5' sequence of *dep1b* is not complete and therefore the number of Fibronectin type III like repeats in Dep1b remains to be determined. Sequence alignments of the PTP domain of Dep1a and Dep1b show highest homology to human Dep1 (data not shown). The catalytic domains of Dep1a and Dep1b have 68% and 65% sequence identity with human Dep1, respectively. We have identified other R3 subfamily members in zebrafish, including PTPβ (Zv6, ENSDARG00000006391) and SAP-1 (Zv6, ENSDARG00000063620). A phylogenetic tree illustrates that indeed Dep1a and Dep1b resemble mammalian Dep1s more than the other R3 subfamily members, PTPβ and SAP-1 (Fig. 1A). Moreover, comparison of synteny between the zebrafish *dep1s* and human *PTPRJ*, encoding Dep1, indicated that both *dep1* genes have the same flanking genes as human *PTPRJ* and thus that *dep1a* and *dep1b* indeed are orthologs of human *PTPRJ* (Fig. 1B).

We obtained the full length *dep1a* cDNA by RT-PCR from 3 dpf zebrafish embryos. Five overlapping fragments were obtained by PCR, based on the ENSEMBL prediction of the gene. We assembled these fragments and generated the full length 4953 bp coding sequence of *dep1a*. In addition, we obtained a fragment of *dep1b* by RT-PCR, encoding the catalytic PTP domain.

We used fragments of *dep1a* and *dep1b*, encompassing the catalytic PTP domains as probes for *in situ* hybridization to establish the expression patterns of *dep1a* and *dep1b*. We found that both genes were maternally expressed (4 cell stage) and displayed ubiquitous expression at early stages of development, 4 hpf and 30 hpf (Figs. 1C–H). Sections of 30 hpf and 48 hpf embryos demonstrated that *dep1a* and *dep1b* are widely expressed in muscles, the neural tube and vascular endothelial cells (Figs. 1I–L). Several other *dep1a*-specific probes were generated using more 5' sequences and *in situ* hybridizations using these probes resulted in similar expression patterns as with the *dep1a* PTP domain probe (data not shown). Since we detected expression of *dep1b*, we conclude that this is a *bona fide* gene and not a pseudogene. Control sense riboprobes for *dep1a* and *dep1b* did not result in specific staining (data not shown). Taken together, our results demonstrate that the zebrafish genome encodes two *dep1* genes that are both expressed ubiquitously during early zebrafish development.

Dep1a-MO induced blood circulation defects

To study the function of Dep1a during zebrafish development, we targeted Dep1a expression using specific morpholinos (MOs). We designed two splice site MOs, directed at exon 21 and exon 22, well upstream of the catalytic site cysteine, Dep1a-MO1 and Dep1a-MO2, respectively (Fig. 2A). We tested the efficacy of these MOs by RT-PCR using exon-specific primers on total RNA from non-injected control embryos and embryos injected with Dep1a-MO1 or Dep1a-MO2. Both

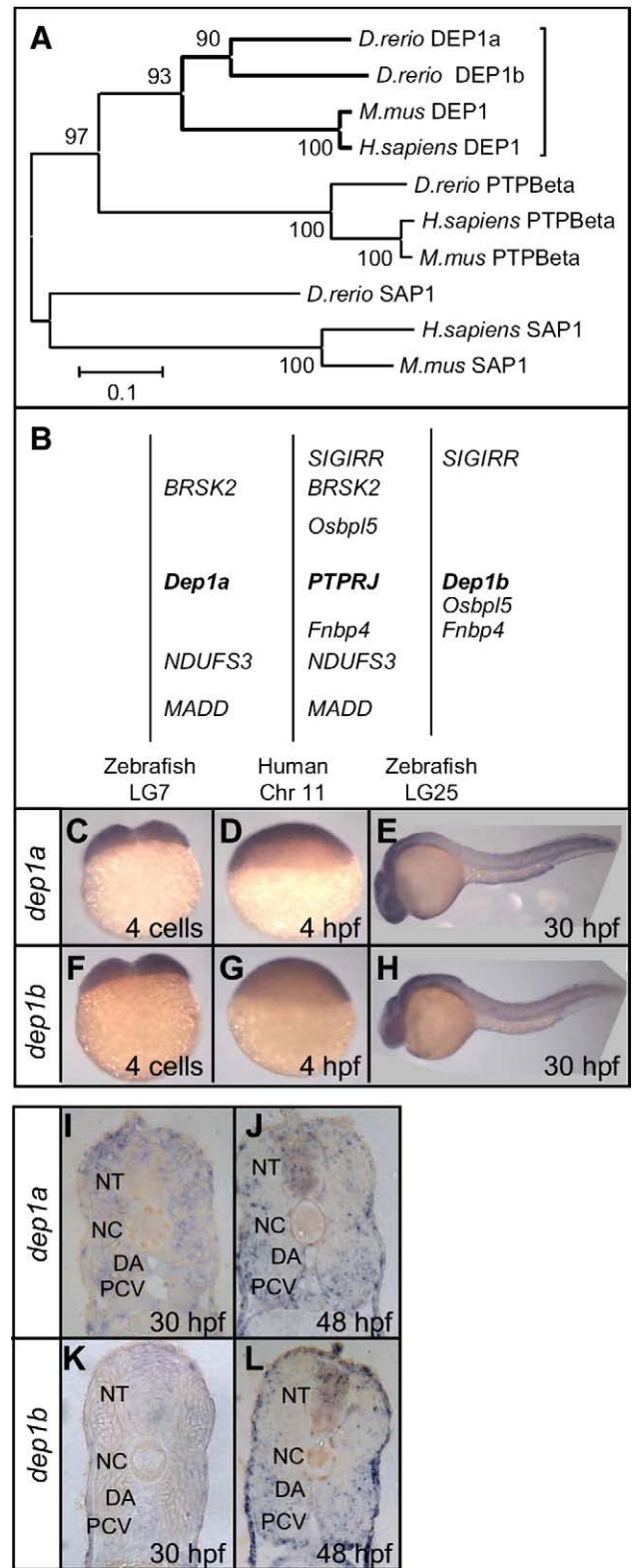


Fig. 1. Dep1a and Dep1b are orthologs of human Dep1 and are broadly expressed during early development. (A) Phylogenetic tree of Dep1 and its most closely related family members, PTPβ and SAP1. The PTP domains of zebrafish (*D. rerio*), human (*H. sapiens*) and mouse (*M. mus*) R3 subfamily members were plotted, based on sequence identity. (B) Genomic localization of human Dep1 (Chr. 11), Dep1a (LG7) and Dep1b (LG25) and genes in their immediate surroundings. (C–L) *Dep1a*- and *dep1b*-specific riboprobes, encompassing the catalytic domain, were generated and used in whole-mount *in situ* hybridization. Whole-mount expression of *dep1a* (C–E) and *dep1b* (F–H) during early zebrafish development, 4 cell stage (C,F), 4 hpf (D,G) and 30 hpf (E,H) are depicted as well as sections of 30 hpf and 48 hpf embryos (I–L). Relevant structures were labeled: DA, dorsal aorta; NC, notochord; NT, neural tube; PCV, posterior cardinal vein.

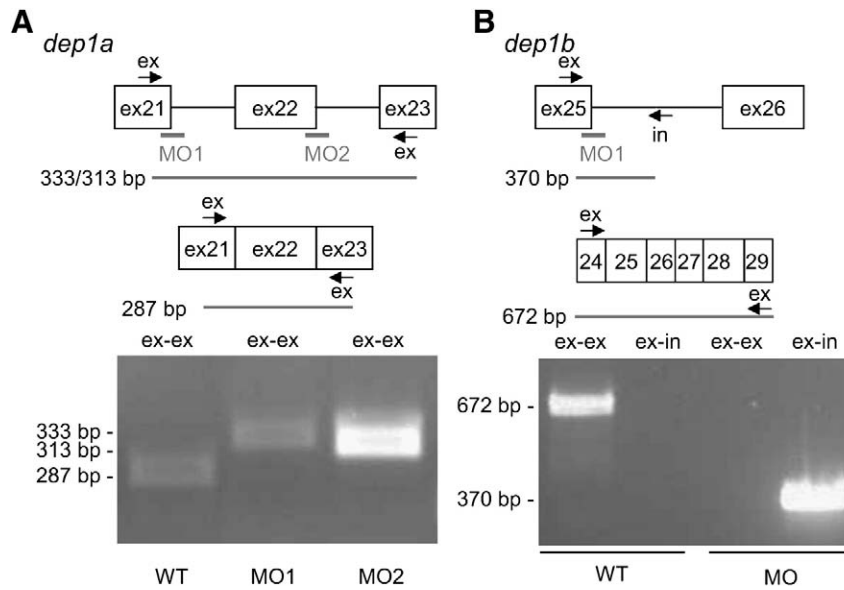


Fig. 2. Dep1a- and Dep1b-MOs efficiently blocked splicing. (A) Dep1a-MO1 and Dep1a-MO2 target the 3' end of exon 21 and exon 22, respectively. Exon-specific primers were designed in exon 21 and exon 23, allowing PCR of spliced RNA (287 bp) and improperly spliced mRNA (333 bp and 313 bp), respectively. RT-PCR was done on non-injected control (WT), Dep1a-MO1 and Dep1a-MO2-injected embryos. The sizes of the obtained PCR fragments on an agarose gel are indicated. (B) The Dep1b-MO targets the 3' end of exon 25, which encodes sequences corresponding to exon 21 of *dep1a* (see also Supplementary Fig. S1). Oligos were designed against exon 25 and intron 25, allowing PCR of unspliced *dep1b* RNA (370 bp) and as a control, exon-specific primers were used (672 bp). RT-PCR was done on RNA, isolated from non-injected control (WT) and Dep1b-MO-injected embryos and the resulting agarose gel is shown with the sizes of the bands indicated.

MOs efficiently blocked splicing, illustrated by the slower migrating bands of 333 bp and 313 bp, respectively, and the absence of the fully spliced, mature RNA band of 287 bp (Fig. 2A). We confirmed that the slower migrating band represented unspliced RNA by sequencing (data not shown). Translation of the unspliced RNAs would result in premature stops and thus truncation of Dep1a, well upstream of the catalytic site cysteine (Supplementary Fig. S1). We tried to detect Dep1a protein in zebrafish embryo lysates by immunoblotting using anti-human Dep1 antibodies and using antibodies that we generated using zebrafish Dep1a catalytic domain as antigen. Unfortunately, these antibodies did not allow us to detect endogenous Dep1 protein in zebrafish (data not shown).

Morphological examination of embryos injected with Dep1a-MO1 indicated that blood circulation was defective at 30 hpf. Notably, *O*-dianisidine staining demonstrated that blood accumulated in the posterior cardinal vein (PCV) (asterisk in Fig. 3B). Blood flow was reduced or absent through the dorsal aorta (DA) and blood accumulated at the aortic bifurcation (arrow in Fig. 3B). Morphological

assessment of embryos injected with Dep1a-MO2 also indicated reduced blood circulation through the axial vasculature (data not shown). These observations contrast with the non-injected control, where the blood is found mainly in the sinus venosus (SV) and in the heart (Fig. 3A). It is noteworthy that injection of non-related morpholinos, such as the Nacre-MO that induces pigmentation defects, did not induce blood circulation defects (data not shown), suggesting that the Dep1a-MO-induced defects were specific.

To investigate whether vasculogenesis was affected by Dep1a knockdown, we micro-injected the Dep1a-MOs into *fli1a::egfp1* transgenic embryos that express GFP in all endothelial cells (Lawson and Weinstein, 2002). Micro-injection of either Dep1a-MO1 or Dep1a-MO2 did not induce apparent defects in vasculogenesis at 30 hpf (Figs. 3C–E). The overall vasculature appeared to be normal with clearly distinguishable dorsal aorta, PCV and intersegmental vessels (Figs. 3C–E). Therefore, the observed accumulation of blood cells and defects in blood circulation as a result of Dep1a knockdown were not the result of gross defects in vasculogenesis.

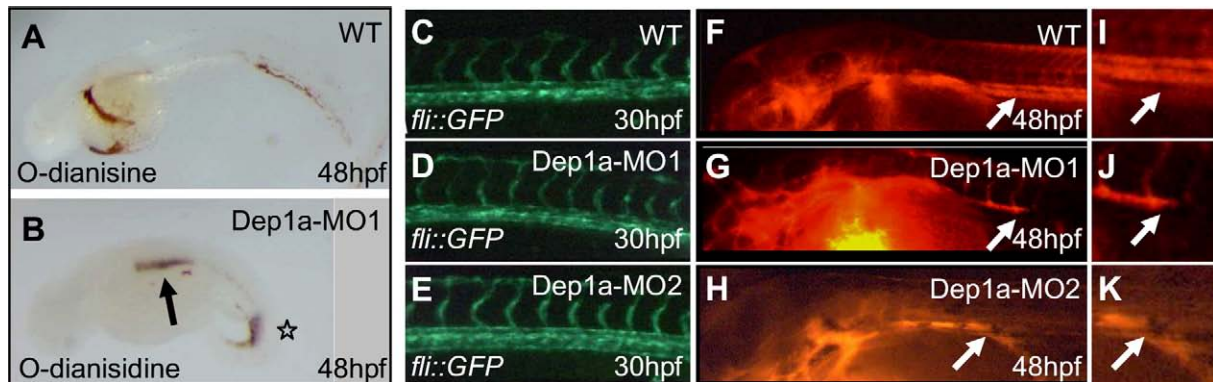


Fig. 3. Dep1a-MO induced blood circulation defects, but vasculogenesis appeared normal. *O*-dianisidine staining of hemoglobin was done on wild type (A) and Dep1a-MO1 (B) injected embryos at 48 hpf. The arrow indicates hemorrhages at the aortic bifurcation and the asterisk blood accumulation around the posterior cardinal vein. *Fli1a::egfp1* transgenic zebrafish embryos were injected with Dep1a-MO1 (D) or Dep1a-MO2 (E) at the 1-cell stage and the vasculature was visualized at 30 hpf. A non-injected *fli1a::gfp1* embryo served as a control (C). Microangiography was done by injection of rhodamine-conjugated dextran into the heart of embryos. Circulation of the dye was visualized using a fluorescence microscope. Non-injected control (F), Dep1a-MO1 injected (G) and Dep1a-MO2-injected embryos (H) all at 48 hpf are depicted here. (J–K) Magnifications of the area where circulation is blocked (arrow).

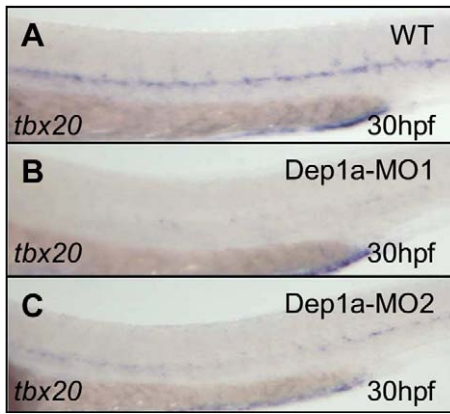


Fig. 4. Dep1a-MO induced reduction in dorsal aorta marker *tbx20*. (A) *In situ* hybridization showing *tbx20* expression in wild type zebrafish embryo at 30 hpf and in Dep1a-MO1 (B) or Dep1a-MO2 (C) injected embryos.

To assay the functionality of the vessels, microangiography was performed by injection of fluorescent rhodamine dextran. In wild type embryos, fluorescence was detected throughout the entire aorta at 48 hpf (Figs. 3F, I). The microangiograms of Dep1a-MO1-injected embryos showed defects at 48 hpf in the axial vasculature. Rhodamine dextran staining was only found anterior to the aortic bifurcation and no fluorescence was detected in the posterior aorta (Figs. 3G, J). Dep1a-MO2 similarly affected functionality of the vasculature, as shown by the microangiogram of wild type embryos, injected with Dep1a-MO2, in which the rhodamine dextran did not reach the posterior part of the embryo (Figs. 3H, K). These experiments indicate that Dep1a appears not to be required for vasculogenesis *per se*, but is essential for functionality of blood vessels at 48 hpf.

To determine the nature of the defects that induced defective blood circulation, we investigated expression of *tbx20*, a dorsal aorta marker (Ahn et al., 2000). *In situ* hybridization using a *tbx20* specific probe confirmed labeling of the dorsal aorta at 30 hpf (Fig. 4A). *Tbx20* expression was reduced in both Dep1a-MO1- and Dep1a-MO2-injected embryos (Figs. 4B, C). The reduction in *tbx20* expression was variable. We classified the defects in *tbx20* expression in 3 classes: class 1, normal wild type expression in the dorsal aorta; class 2 (mild), patchy expression in some cells and class 3 (severe), *tbx20* expression

completely absent (Fig. 5A). We quantified the number of embryos in each class, based on the classification above and found that a significant proportion of the injected embryos displayed reduced *tbx20* expression (Fig. 5B, Supplementary Table S1).

To establish that the observed defects were specific, we performed rescue experiments. Rescue experiments are usually done by co-injection of MOs with synthetic RNA encoding the target protein. *In vitro* synthesis of RNA encoding Dep1a did not yield sufficient RNA for the co-injections. Therefore, we co-injected a CMV promoter-driven expression vector for zebrafish Dep1a. This led to a significant reduction in the number of embryos with aberrant *tbx20* expression (Fig. 5B). The expression vector by itself did not affect *tbx20* expression in injected embryos (Supplementary Table S1). The expression vector for zebrafish Dep1a contained a Myc epitope tag immediately following the signal sequence, facilitating detection of transgene expression. We transfected the Myc-tagged expression vector for Dep1a into COS-1 cells and established its expression by immunoblotting. As controls, we used Myc-tagged RPTP α and control vector. As shown in Fig. 5C, Dep1a was detected as a band of ~250 kDa, using anti-Myc antibodies. Myc-tagged RPTP α was detected as a broad band of ~180 kDa (Blanchetot et al., 2002). In embryos, expression of Myc-tagged Dep1a was not detectable by immunohistochemistry, which was presumably due to low expression levels of Dep1a. Nevertheless, our data demonstrate that full length Dep1a was produced from this expression vector and co-injection with Dep1a-MO rescued the Dep1a knockdown phenotype, indicating that the phenotype was specific.

Dep1a and Dep1b act synergistically in aorta formation

We hypothesized that Dep1a and Dep1b might have redundant functions, because of their high similarity. To investigate this hypothesis, we designed a Dep1b-MO directed at the exon–intron boundary that corresponded to the Dep1a-MO1 target site (see Supplementary Fig. S1). We established that micro-injection of this Dep1b-MO blocked splicing (Fig. 2B). Co-injection of high amounts of the Dep1a- and Dep1b-MOs (8 ng each) induced non-specific defects in the embryos, including necrosis and oedemas (data not shown). Therefore, we reduced the amount of each MO to 4 ng. Micro-injection of 4 ng Dep1a-MO or Dep1b-MO-induced defects in *tbx20* expression, albeit in a low percentage of the embryos (Figs. 6A–C, I,

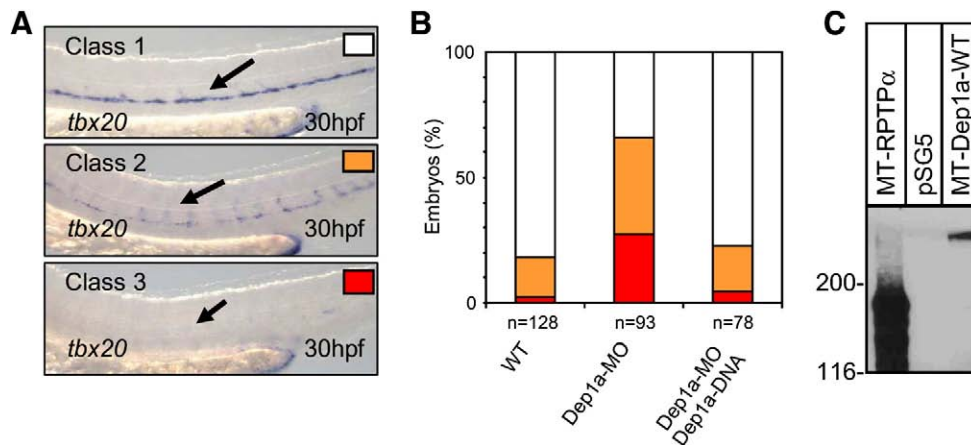


Fig. 5. Dep1a-MO-induced reduction in *tbx20* expression was specific. (A) Classification of the observed defects after Dep1a-MO injection (8 ng/embryo): upper panel, no effect, normal *tbx20* expression (white), middle panel, mild effect, patchy *tbx20* expression (orange), lower panel, severe effect, no *tbx20* expression (red). (B) Quantification of the effects of Dep1a knockdown. The percentages of embryos in the three different classes is given in control embryos (WT) and in Dep1a-MO1 (8 ng) injected embryos. Moreover, Dep1a-MO1 was co-injected with a CMV promoter-driven expression vector for Dep1a (12.5 ng), effectively rescuing the defects. Total numbers of embryos from at least three independent experiments are indicated (n). Exact numbers are given in Supplementary Table S1. (C) Expression vectors for Myc epitope tagged Dep1a and – as a control – for RPTP α were transfected into COS cells. The cells were lysed and whole cell lysates were run on a 7.5% SDS-PAGE gel. The material on the gel was blotted and the blots were probed with anti-Myc MAb 9E10. An immunoblot is depicted developed with enhanced chemiluminescence and the positions of marker proteins that were co-electrophoresed with the sample are indicated in kDa on the left.

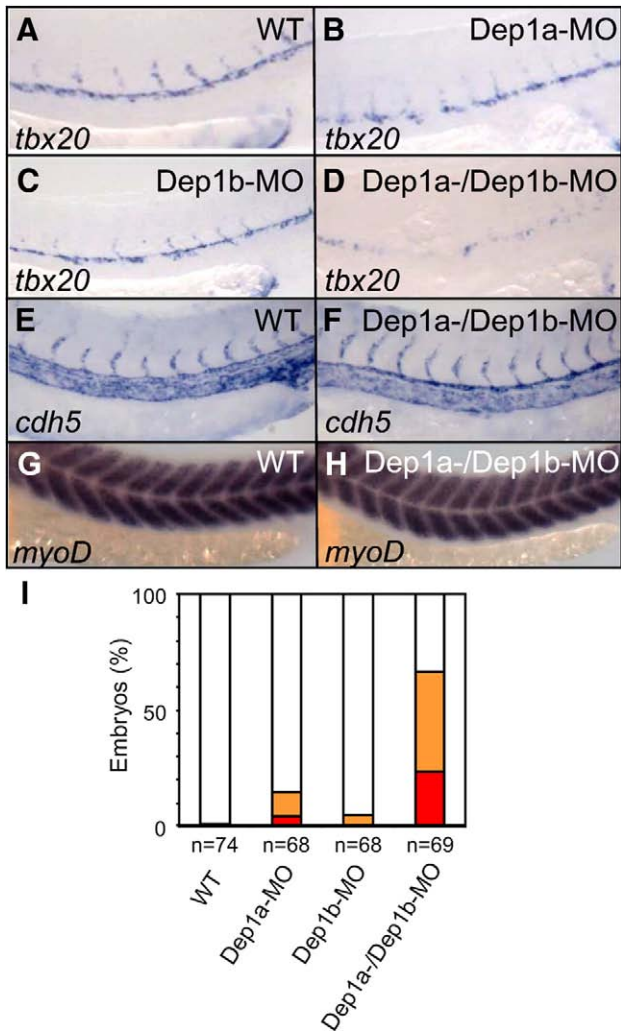


Fig. 6. Synergistic effects of Dep1a and Dep1b MOs. Dep1a- and Dep1b-MOs were (co-) injected at the 1-cell stage (4 ng each) and the embryos were fixed at 30 hpf. *In situ* hybridizations were done using *tbx20* specific probes (A–D), a *cdh5* (*ve-cadherin*)-specific probe (E,F) or *myoD*-specific probes (G,H). (I) Quantification of defects in *tbx20* expression, classified as outlined in Fig. 5. The total number of embryos that was analyzed for each condition from three independent experiments is indicated here and depicted in Supplementary Table S2.

Supplementary Table S2). However, co-injection of Dep1a- and Dep1b-MOs strongly enhanced the percentage of embryos with defective *tbx20* expression, indicating that these MOs acted synergistically (Figs. 6D, I; Supplementary Table S2). Co-injection of Dep1a-MO or Dep1b-MO with the non-related Nacre-MO did not lead to an increase in defects in *tbx20* expression (Supplementary Table S2), illustrating that this defect is specifically due to knockdown of the two Dep1 proteins. Interestingly, *cdh5* expression, a marker for vascular endothelial cells, was not affected by injection of both Dep1a-MO and Dep1b-MO (Figs. 6E, F). Moreover, the pattern of the somite marker *myoD* was not affected either, indicating that somitogenesis was not affected by Dep1 knockdown (Figs. 6G, H). Our results indicate that Dep1a-MO and Dep1b-MO induced defects in the dorsal aorta on their own. Moreover, combined, the Dep1a-MO and Dep1b-MO acted synergistically, suggesting that the function of Dep1a and Dep1b is partially overlapping.

Dep1a and Dep1b are required for arterial/venous fate decision

To further investigate the role of Dep1 in blood vessels, we examined the arterial markers *notch5*, *ephrinB2* and *grl/hey2* and the

venous specific markers, *ephB4* and *dab2*. Dep1a/Dep1b-MO injections reduced expression of all three arterial markers (Fig. 7A). *Notch5* expression was almost completely lost from the dorsal aorta where it is normally expressed (Fig. 7A, cf. WT and Dep1a/Dep1b-MO). *EphrinB2* expression persists only in a patchy, non-continuous manner in Dep1a/Dep1b morphants, whereas in non-injected control embryos, *ephrinB2* is expressed in a continuous line in the dorsal aorta (Fig. 7A). Similarly, *grl* expression is almost completely lost from the Dep1a/Dep1b-MO-injected embryos. This panel of arterial markers suggests that arteries do not form properly.

The venous *ephB4* and *dab2* markers stain the PCV in the trunk of wild type non-injected control embryos. *EphB4* staining was expanded in Dep1a/Dep1b morphants, compared to non-injected controls. Moreover, the PCV appeared to be slightly enlarged (Fig. 7B). Similarly, *dab2* staining was expanded and the PCV was enhanced. It appeared that *ephB4* and *dab2* were expressed where the dorsal aorta is localized normally. Together, the venous and arterial markers demonstrate that Dep1a/Dep1b-MOs induced a decrease in arterial marker expression and a concomitant increase in venous marker expression. These results suggest that Dep1a and Dep1b have a role in the arterial cell fate decision of vascular endothelial cells.

The mechanism underlying the role of Dep1 in arterial/venous cell fate decisions

Much work has been done on how the arterial/venous cell fate is established. The model that is emerging is that *sonic hedgehog* (*shh*) from the notochord induces *vegf* in somites, which in turn induces *notch5* and *flk1* in endothelial cells to induce arterial differentiation (Lawson et al., 2002). *Notch5* induces *ephrinB2* and *grl* expression and inhibits *flt4*. *Grl* mutant zebrafish display selectively perturbed artery formation (Zhong et al., 2000) and the arterial/venous cell fate decision is guided by *grl* (Zhong et al., 2001). Interestingly, the *grl*

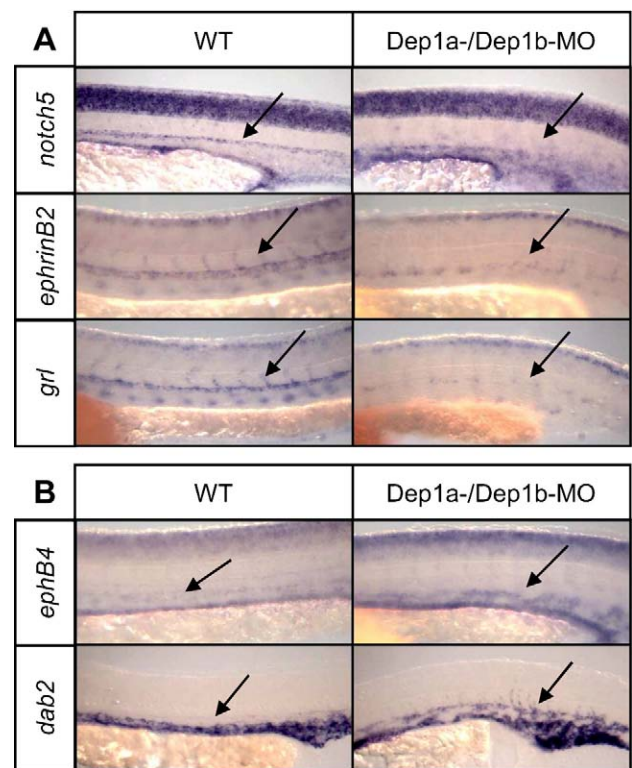


Fig. 7. Dep1-MO induced reduction in arterial cell fate. Dep1a- and Dep1b-MOs were co-injected and the embryos were fixed at 30 hpf. Three arterial markers (*notch5*, *ephrinB2* and *grl*) and two venous markers (*ephB4* and *dab2*) were used for *in situ* hybridizations. The position of the dorsal aorta is indicated with an arrow.

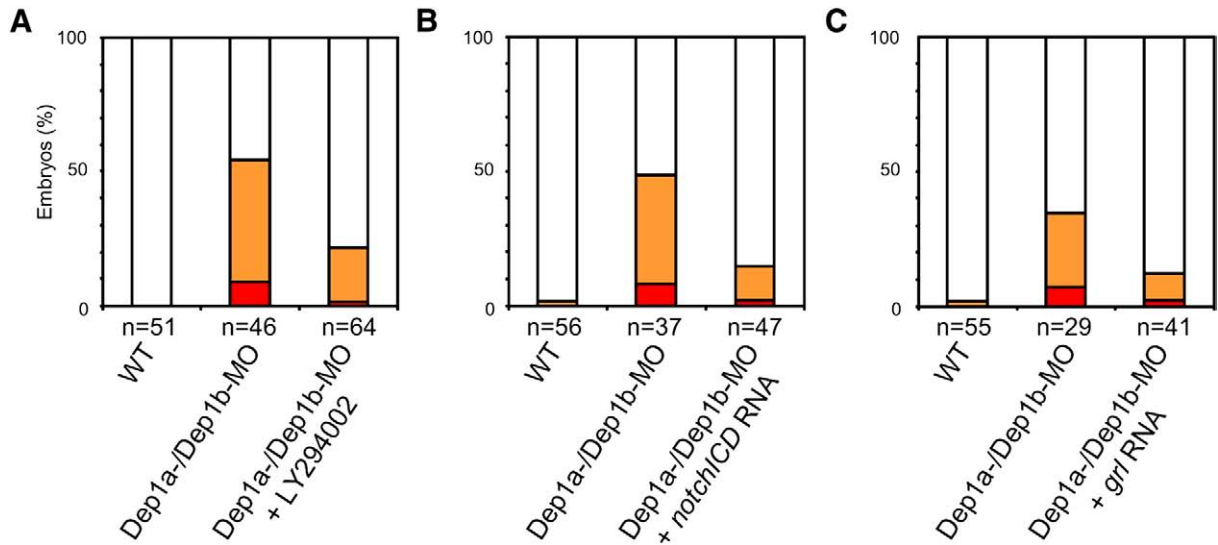


Fig. 8. Rescue of Dep1 morphant phenotype by PI-3K inhibitor and expression of *notch1CD* and *grl*. Effects of (co-)injection on arterial differentiation were assessed by *in situ* hybridization, using a *tbx20*-specific probe. Rescues were done using the PI-3K inhibitor LY294002 (A), *notch1CD* RNA (B) and *grl* RNA (C). The total numbers of embryos that were used for each condition from three independent experiments are indicated (n) and are given in Supplementary Table S3.

phenotype is highly reminiscent of the Dep1a/Dep1b knockdown phenotype, in that *grl* mutants also show reduced arterial markers (*ephrinB2*) and enhanced venous markers (*ephB4*) (Zhong et al., 2001). We reproduced the *grl* phenotype using Grl-MOs and compared the *grl* and Dep1a/Dep1b phenotypes side by side and found that the Dep1 knockdown is a phenocopy of the *grl* knockdown (data not shown). This may suggest that Dep1a/Dep1b acted through a similar mechanism. In fact, we demonstrated that *grl* and *notch5* expression are strongly reduced in Dep1a/Dep1b knockdowns, indicating that Dep1a/Dep1b are genetically upstream of *notch* and *grl*. Phosphatidylinositol-3 kinase (PI3K) inhibitors were identified in a screen for suppressors of the *grl* mutant phenotype and PI3K inhibitors promote arterial specification (Hong et al., 2006).

We set out to address the mechanism underlying Dep1a/Dep1b signaling by analysis of the potential to rescue the Dep1a/Dep1b-MO-induced decrease in *tbx20* expression by interference with known *grl* signaling components. To this end, we used LY294002, a specific PI3K inhibitor, which rescued the Dep1a/Dep1b induced phenotype (Fig. 8A; Supplementary Table S3), similar to LY-mediated rescue of the *grl* phenotype (Hong et al., 2006). Co-injection of RNA encoding Notch intracellular domain (*notch1CD*) rescued the Dep1a/Dep1b-MO-induced decrease in *tbx20* expression (Fig. 8B; Supplementary Table S3). Finally, the Dep1a/Dep1b knockdown was rescued by *grl* RNA injection as well (Fig. 8C; Supplementary Table S3). Control *gfp* RNA co-injections with Dep1a/Dep1b-MOs did not affect *tbx20* expression (data not shown). These results demonstrate that Dep1a/Dep1b signaling counteracts PI3K signaling and is mediated by *notch* and *grl* expression.

Discussion

Here, we provide evidence that the zebrafish orthologs of Dep1, Dep1a and Dep1b, act in arterial cell fate decision. We found that inhibition of PI3K and expression of *notch1CD* and *grl* rescued Dep1a/Dep1b morphants, providing an underlying mechanism for the function of Dep1.

Mouse mutants in which part of the catalytic domain of Dep1 was replaced by GFP die at midgestation, before embryonic day 11.5. Homozygous mutant embryos were indistinguishable from wild type mice at embryonic day 8.5 in the gross appearance of the rostral-caudal-dorsal aorta, anterior and posterior cardinal veins, vitelline artery and vein and yolk sac capillary plexus. Therefore, Dep1

appeared not to be required for early embryonic vasculogenesis. However, by day 9, a collapse of the dorsal aorta was observed accompanied by the presence of abundant endothelial cells. At embryonic day 9.5, the dorsal aorta appeared as a disorganized string of aligned endothelial cells and at embryonic day 10.5, its outline was discontinuous (Takahashi et al., 2003). Surprisingly, deletion of exons 3, 4 and 5 of Dep1 did not affect embryonic development and Dep1^{-/-} mice were viable and fertile (Trapasso et al., 2006). There is an obvious discrepancy in phenotypes between these two Dep1 mutant mouse models, which may be due to the fact that the two mouse models are inherently different. The knock out mice apparently do not express Dep1 protein (Trapasso et al., 2006). Yet, the Dep1-GFP fusion protein is expressed (Takahashi et al., 2003). Therefore, the Dep1-GFP fusion protein may function by itself, albeit it lacks catalytic activity.

The zebrafish knockdown phenotype was reminiscent of the phenotype in mice in which the catalytic domain of Dep1 was replaced by *gfp* sequences. The Dep1-MOs induced varying degrees of reduction of the dorsal aorta marker, *tbx20*. Moreover, we have observed that the dorsal aorta in sections of Dep1a/Dep1b-MO-injected embryos apparently did not lumenize, which was accompanied by an enlarged PCV (data not shown). Our data suggest that arterial differentiation was reduced in Dep1 morphants, which was accompanied by ectopic expression of venous markers. This phenotype was reminiscent of the *grl* mutant phenotype (Weinstein et al., 1995; Zhong et al., 2001). We reproduced the *grl* phenotype by Grl-MO injection and found that indeed, Dep1a/Dep1b morphants phenocopied the Grl knockdown. Analysis of epigenetic interactions indicated that co-injection of Dep1-MOs with Grl-MO was additive, as assessed by *tbx20* expression (data not shown). Importantly, Dep1-MOs abolished *grl* expression in the dorsal aorta, suggesting that Dep1 acts upstream in a signaling pathway regulating *grl* expression. *Grl* RNA injection was sufficient to rescue Dep1a/Dep1b knockdown, confirming that Dep1 and Grl interact genetically. Moreover, expression of *notch5* was reduced in Dep1a/Dep1b morphants and RNA encoding Notch1CD, a known factor upstream of *grl*, rescued Dep1a/Dep1b-MO injection. Finally, we demonstrated that the PI3K inhibitor LY294002 that was reported to rescue the *grl* phenotype, also rescued the Dep1a/Dep1b knockdown phenotype. Our data firmly place Dep1 upstream in a cascade, involving PI3K, *notch* and *grl*.

The soluble factor VEGF is an important regulator of arterial/venous cell fate decisions (Lawson et al., 2002). Dep1 may act directly on VEGFR2 signaling, as it has been demonstrated in tissue culture

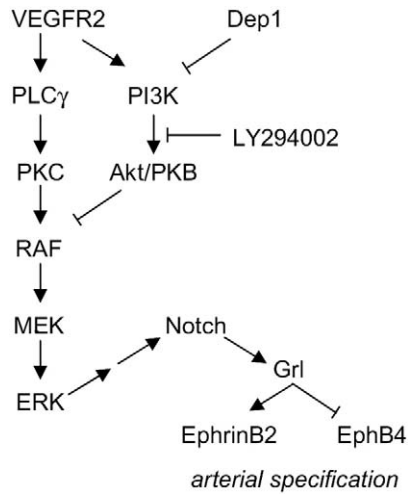


Fig. 9. Model for the role of Dep1 in arterial specification. Dep1 may act at or upstream of PI3K, inhibiting Akt/PKB activation, thus relieving inhibition of the RAF–MEK–ERK pathway. This pathway regulates expression of Notch and Grl, positive regulators of the arterial marker, EphrinB2, and negative regulators of venous EphB4. Absence of Dep1 was rescued by PI3K inhibitor (LY294002) and by expression of Notch and Grl.

cells that downregulation of Dep1 results in enhanced VEGFR2 phosphorylation (Lampugnani et al., 2003). Whether Dep1 acts through VEGFR2 signaling in arterial differentiation during zebrafish development remains to be determined.

In *C. elegans*, the Dep1 ortholog is involved in cell fate decisions in vulval development. Dep1 inhibits the primary cell fate specification in the future secondary cells by induction of the transcription of a set of inhibitors of the EGFR/RAS/MAPK signaling pathway (Berset et al., 2005). Our data suggest that Dep1 has a role in cell fate decisions in zebrafish as well, in that Dep1 is required for arterial specification. Interestingly, Notch signaling is repressed in the primary cells in *C. elegans* and acts in parallel to Dep1 in secondary cells. Similarly, Notch is expressed in the dorsal aorta in zebrafish, but not in venous cells, suggesting it has a similar decisive role in cell differentiation as in *C. elegans*. However, in zebrafish, Dep1-MO injections result in loss of *notch5* expression in future dorsal aorta cells and *notch1CD* expression rescued Dep1 morphants, indicating that Dep1 acts upstream of Notch in arterial cell differentiation, not in parallel to Notch as in *C. elegans*. Nevertheless, there are parallels between Dep1 signaling in *C. elegans* and in zebrafish, in that Dep1 has a decisive role in cell fate determination.

Taken together, our data suggest a model that builds on previous models for the role of Dep1 in cell specification (Berset et al., 2005; Hong et al., 2006) in which Dep1 acts at the level of PI3K or upstream (Fig. 9). Inhibition of PI3K by Dep1 relieves inhibition of the RAF–MEK–ERK pathway which controls Notch and Grl expression and thus arterial specification. In the absence of Dep1, arterial specification is reduced, which is rescued by the PI3K inhibitor LY294002 and by expression of Notch and Grl, restoring the pathway (Fig. 9).

Our results indicate that zebrafish Dep1 acted in arterial cell fate determination and we provide evidence that Grl and Notch were involved. Future work should focus on whether Dep1 acts on the VEGFR2–RAF–MEK–ERK signaling pathway.

Materials and methods

Zebrafish lines and maintenance

Zebrafish were maintained and staged according to standard protocols (Westerfield, 1995). The zebrafish lines we used are the ABTL strains and the transgenic line *fli1a::egfp* (Lawson and Weinstein, 2002).

Cloning of zebrafish Dep1a and Dep1b sequences

To identify the zebrafish Dep1 orthologue, a BLAST search of human Dep1 protein (SWISSPROT number: Q12913) against the zebrafish translated database (tblastn) Zv6 Ensembl genome assembly was performed (www.ensembl.org). Two genes encoding Dep1 protein, Dep1a, in LG7 at position 51.7 Mb (ENSARG00000011567) and Dep1b, LG25 at position 22.2 Mb (ENSARG00000033042), were identified. Full length Dep1a was amplified from 3 dpf zebrafish cDNA generated by oligo d(T) using standard PCR conditions. Five overlapping PCR products, covering the entire predicted cDNA of Dep1a were amplified and subcloned in pBluescript SK+. The sequence was verified and all five clones were assembled together in pCS2+ plasmid. The Dep1a coding sequence without its signal sequence was fused in-frame to the signal sequence of RPTPα and in-frame Myc-tag (Blanchetot et al., 2002), allowing expression of Myc-tagged transmembrane proteins. A fragment of Dep1b (660 bp) encompassing the PTP domain was amplified from a 2 dpf zebrafish total RNA by RT-PCR. The fragment was then subcloned in pBluescript SK+ and verified by sequencing.

Phylogenetic reconstruction

As input for the MEG3.1 program (Molecular Evolutionary Genetics Analysis, version 3.1), we used protein sequences of the PTP domain of human Dep1 (Swissprot Q12913), mouse Dep1 (Swissprot Q64455), zfDep1a and zfDep1b (ENSARG00000011567 and ENSARG00000033042), human PTPβ (Swissprot P23476), mouse PTPβ (NM_029928), zfPTPβ (ENSARG00000006391), human SAP1 (Swissprot Q15426), mouse SAP1 (NP_997153) and zfPTPSAP1a (ENSARG000000063620). The protein sequences from zebrafish PTPβ and zebrafish SAP1 were found by blasting their human homologues against the zebrafish Zv6 Ensembl genome assembly. The phylogenetic tree was built with Neighbor-joining algorithm with a pair-wise deletion option and using Dayhoff Matrix Model. Support for each node was determined by a bootstrap test.

In situ hybridization

Whole-mount *in situ* hybridizations were performed essentially as described (Thisse et al., 1993) except for the Dep1a and Dep1b *in situ* hybridizations in which the staining was developed in staining buffer containing polyvinylalcohol (PVA) (100 mM tris–HCl pH=9.5, 100 mM NaCl, 0.1% Tween, 50 mM MgCl₂, 10% PVA, 0.17 mg/ml NBT, 0.17 mg/ml BCIP). The probes we used have been described before: *tbx20* (Ahn et al., 2000), *cdh5/ve-cad* (Larson et al., 2004), *myoD* (Weinberg et al., 1996), *notch3/5* (Gering and Patient, 2005), *ephrinB2a* and *ephB4* (Cooke et al., 2001), *dab2* (Song et al., 2004), *grl* (Zhong et al., 2000). We used fragments of *dep1a* and *dep1b*, encompassing the catalytic PTP domains as probes for *in situ* hybridization.

Morpholinos, RNA and injections

Antisense MOs were designed to target exon–intron splice sites of genomic Dep1a and Dep1b and ordered from GeneTools (Philomath, OR, USA):

Dep1a-MO1 5′-TGAGGTTCTACATGGCAGCACATT
 Dep1a-MO2 5′-TTTCACTTCTACCGCATGTAGTT
 Dep1b-MO1 5′-GAAGATACTACAAGGTAACATT.

Morpholinos were diluted in 1×Danieau buffer (58 mM NaCl, 0.7 mM KCl, 0.4 mM MgSO₄, 0.6 mM Ca(NO₃)₂, 5 mM Hepes pH 7.6) and 1 nl was injected into embryos at 1–2 cell stage in concentrations ranging from 1–15 ng/nl. mMESAGE mMACHINE kit (Ambion, Austin, TX, USA) was used to synthesize 5′ capped sense RNAs for full length *grl* (RZPD, Berlin, Germany) and *notch1CD* (gift of Dana Zivkovic).

Range of plasmid DNA (Dep1a-CS, Dep1a-ED, Dep1a-FL) (1–25 pg/ml) or synthetic RNA (0.5–50 pg/ml) were (co-)injected into 1 cell stage embryos and phenotypes were assessed at the indicated stages.

RT-PCR

Total RNA from 2 dpf-old wild type and MO-injected embryos (Dep1aMO1: 4 ng/ml, Dep1aMO2: 12 ng/ml, Dep1bMO: 8 ng/ml) was isolated using guanidine isothiocyanate (GIT) method. Following DNase treatment (Ambion, Austin, TX, USA) of the total RNA, reverse transcription was done using M-MLV-RT (Isogen, IJsselstein, the Netherlands) and subsequently, PCR was done using standard protocols, using appropriate oligonucleotides.

O-dianisidine staining

O-dianisidine (Sigma-Aldrich, St. Louis, MO, USA) was used to detect hemoglobin exactly as described previously (Kawahara and Dawid, 2001).

Microangiography

Rhodamine-conjugated dextran (Tetramethylrhodamine, 2,000,000 MW, Invitrogen, Carlsbad, CA, USA) was injected in the heart of embryos slightly anaesthetized with tricaine (MS222) and mounted in 0.8% low melting agarose (Isogai et al., 2001). Fluorescent dextran was visualized using a Leica fluorescence microscope.

PI-3 kinase inhibitor LY 294002

Embryos were grown in embryo medium and at 4 hpf various concentrations of LY 294002 inhibitor (Calbiochem, San Diego, CA, USA) ranging from 2.5 to 15 μ M were added. Control embryos were incubated with equal amounts of solvent (DMSO). Embryos were scored at 30 hpf by fixing and *in situ* hybridization using a *tbx20* specific probe.

Transfections

COS-1 cells were grown in Dulbecco's modified Eagle's medium/F12 supplemented with 7.5% Fetal Calf Serum. Dep-1 constructs were transfected by calcium phosphate precipitation as described previously. Cells were harvested by lysis in 50 mM HEPES pH 7.5, 150 mM NaCl, 1.5 mM MgCl₂, 1 mM EGTA, 10% glycerol, 1% Triton X-100, 1 mM aprotinin, 1 mM leupeptin, and 1 mM *ortho*-vanadate. Cell lysates were cleared and an aliquot was boiled in equal volume 2 \times Laemmli Sample Buffer and run on a 7.5% SDS-PAGE gel. Proteins were subsequently transferred by semi-dry blotting to a PVDF membrane. Immunoblotting was done using standard protocols. The blots were probed with anti-Myc monoclonal antibody 9E10 and with affinity purified anti-zebrafish Dep1a antibody that we raised against a GST-fusion protein encoding the catalytic domain of Dep1a. The immunoblots were visualized by Enhanced Chemiluminescence (ECL).

Acknowledgments

The authors would like to thank various members of the zebrafish community for the generous gifts of molecular marker probes and members of the lab for technical support. In particular, we would like to thank Vincent Runtuwene for micro-injections. This work was supported in part by an EU research training network (HPRN-CT-2000-00085).

Appendix A. Supplementary data

Supplementary data associated with this article can be found, in the online version, at doi:10.1016/j.ydbio.2008.09.011.

References

- Ahn, D.G., Ruvinsky, I., Oates, A.C., Silver, L.M., Ho, R.K., 2000. *tbx20*, a new vertebrate T-box gene expressed in the cranial motor neurons and developing cardiovascular structures in zebrafish. *Mech. Dev.* 95, 253–258.
- Alonso, A., Sasin, J., Bottini, N., Friedberg, I., Friedberg, I., Osterman, A., Godzik, A., Hunter, T., Dixon, J., Mustelin, T., 2004. Protein tyrosine phosphatases in the human genome. *Cell* 117, 699–711.
- Andersen, J.N., Jansen, P.G., Echwald, S.M., Mortensen, O.H., Fukada, T., Del Vecchio, R., Tonks, N.K., Moller, N.P., 2004. A genomic perspective on protein tyrosine phosphatases: gene structure, pseudogenes, and genetic disease linkage. *FASEB J.* 18, 8–30.
- Berset, T.A., Hoier, E.F., Hajnal, A., 2005. The *C. elegans* homolog of the mammalian tumor suppressor Dep-1/Sccl1 inhibits EGFR signaling to regulate binary cell fate decisions. *Genes Dev.* 19, 1328–1340.
- Blanchetot, C., Tertoolen, L.G., Overvoorde, J., den Hertog, J., 2002. Intra- and intermolecular interactions between intracellular domains of receptor protein-tyrosine phosphatases. *J. Biol. Chem.* 277, 47263–47269.
- Borges, L.G., Seifert, R.A., Grant, F.J., Hart, C.E., Disteche, C.M., Edelhoff, S., Solca, F.F., Lieberman, M.A., Lindner, V., Fischer, E.H., Lok, S., Bowen-Pope, D.F., 1996. Cloning and characterization of rat density-enhanced phosphatase-1, a protein tyrosine phosphatase expressed by vascular cells. *Circ. Res.* 79, 570–580.
- Cooke, J., Moens, C., Roth, L., Durbin, L., Shiomi, K., Brennan, C., Kimmel, C., Wilson, S., Holder, N., 2001. Eph signalling functions downstream of Val to regulate cell sorting and boundary formation in the caudal hindbrain. *Development* 128, 571–580.
- de la Fuente-Garcia, M., Nicolas, J.M., Freed, J.H., Palou, E., Thomas, A.P., Vilella, R., Vives, J., Gaya, A., 1998. CD148 is a membrane protein tyrosine phosphatase present in all hematopoietic lineages and is involved in signal transduction on lymphocytes. *Blood* 91, 2800–2809.
- den Hertog, J., 1999. Protein-tyrosine phosphatases in development. *Mech. Dev.* 85, 3–14.
- Gering, M., Patient, R., 2005. Hedgehog signaling is required for adult blood stem cell formation in zebrafish embryos. *Dev. Cell* 8, 389–400.
- Hong, C.C., Peterson, Q.P., Hong, J.Y., Peterson, R.T., 2006. Artery/vein specification is governed by opposing phosphatidylinositol-3 kinase and MAP kinase/ERK signaling. *Curr. Biol.* 16, 1366–1372.
- Hunter, T., 1995. Protein kinases and phosphatases: the yin and yang of protein phosphorylation and signaling. *Cell* 80, 225–236.
- Isogai, S., Horiguchi, M., Weinstein, B.M., 2001. The vascular anatomy of the developing zebrafish: an atlas of embryonic and early larval development. *Dev. Biol.* 230, 278–301.
- Kawahara, A., Dawid, I.B., 2001. Critical role of *bik1f* in erythroid cell differentiation in zebrafish. *Curr. Biol.* 11, 1353–1357.
- Keane, M.M., Lowrey, G.A., Ettenberg, S.A., Dayton, M.A., Lipkowitz, S., 1996. The protein tyrosine phosphatase DEP-1 is induced during differentiation and inhibits growth of breast cancer cells. *Cancer Res.* 56, 4236–4243.
- Lampugnani, M.G., Zanetti, A., Corada, M., Takahashi, T., Balconi, G., Breviaro, F., Orsenigo, F., Cattelino, A., Kemler, R., Daniel, T.O., Dejana, E., 2003. Contact inhibition of VEGF-induced proliferation requires vascular endothelial cadherin, beta-catenin, and the phosphatase DEP-1/CD148. *J. Cell Biol.* 161, 793–804.
- Larson, J.D., Wadman, S.A., Chen, E., Kerley, L., Clark, K.J., Eide, M., Lippert, S., Nasevicius, A., Ekker, S.C., Hackett, P.B., Essner, J.J., 2004. Expression of VE-cadherin in zebrafish embryos: a new tool to evaluate vascular development. *Dev. Dyn.* 231, 204–213.
- Lawson, N.D., Weinstein, B.M., 2002. In vivo imaging of embryonic vascular development using transgenic zebrafish. *Dev. Biol.* 248, 307–318.
- Lawson, N.D., Vogel, A.M., Weinstein, B.M., 2002. Sonic hedgehog and vascular endothelial growth factor act upstream of the Notch pathway during arterial endothelial differentiation. *Dev. Cell* 3, 127–136.
- Ostman, A., Yang, Q., Tonks, N.K., 1994. Expression of DEP-1, a receptor-like protein-tyrosine-phosphatase, is enhanced with increasing cell density. *Proc. Natl. Acad. Sci. U. S. A.* 91, 9680–9684.
- Ruivenkamp, C.A., van Wezel, T., Zanon, C., Stassen, A.P., Vlcek, C., Csikos, T., Klous, A.M., Tripodis, N., Perrakis, A., Boerrigter, L., Groot, P.C., Lindeman, J., Mooi, W.J., Meijjer, G.A., Scholten, G., Dauwerse, H., Paces, V., van Zandwijk, N., van Ommen, G.J., Demant, P., 2002. *Ptpn11* is a candidate for the mouse colon-cancer susceptibility locus *Sccl1* and is frequently deleted in human cancers. *Nat. Genet.* 31, 295–300.
- Song, H.D., Sun, X.J., Deng, M., Zhang, G.W., Zhou, Y., Wu, X.Y., Sheng, Y., Chen, Y., Ruan, Z., Jiang, C.L., Fan, H.Y., Zou, L.L., Kanki, J.P., Liu, T.X., Look, A.T., Chen, Z., 2004. Hematopoietic gene expression profile in zebrafish kidney marrow. *Proc. Natl. Acad. Sci. U. S. A.* 101, 16240–16245.
- Takahashi, T., Takahashi, K., Mernaugh, R., Drozdoff, V., Sipe, C., Schoecklmann, H., Robert, B., Abrahamson, D.R., Daniel, T.O., 1999. Endothelial localization of receptor tyrosine phosphatase, ECRTP/DEP-1, in developing and mature renal vasculature. *J. Am. Soc. Nephrol.* 10, 2135–2145.
- Takahashi, T., Takahashi, K., St John, P.L., Fleming, P.A., Tomemori, T., Watanabe, T., Abrahamson, D.R., Drake, C.J., Shirasawa, T., Daniel, T.O., 2003. A mutant receptor tyrosine phosphatase, CD148, causes defects in vascular development. *Mol. Cell Biol.* 23, 1817–1831.
- Thisse, C., Thisse, B., Schilling, T.F., Postlethwait, J.H., 1993. Structure of the zebrafish *snail1* gene and its expression in wild-type, spadetail and no tail mutant embryos. *Development* 119, 1203–1215.
- Trapasso, F., Iuliano, R., Boccia, A., Stella, A., Visconti, R., Bruni, P., Baldassarre, G., Santoro, M., Viglietto, G., Fusco, A., 2000. Rat protein tyrosine phosphatase eta suppresses the neoplastic phenotype of retrovirally transformed thyroid cells through the stabilization of p27(Kip1). *Mol. Cell Biol.* 20, 9236–9246.

- Trapasso, F., Drusco, A., Costinean, S., Alder, H., Aqeilan, R.I., Iuliano, R., Gaudio, E., Raso, C., Zanesi, N., Croce, C.M., Fusco, A., 2006. Genetic ablation of *Ptprj*, a mouse cancer susceptibility gene, results in normal growth and development and does not predispose to spontaneous tumorigenesis. *DNA Cell Biol.* 25, 376–382.
- Weinberg, E.S., Allende, M.L., Kelly, C.S., Abdelhamid, A., Murakami, T., Andermann, P., Doerre, O.G., Grunwald, D.J., Riggleman, B., 1996. Developmental regulation of zebrafish *MyoD* in wild-type, no tail and spadetail embryos. *Development* 122, 271–280.
- Weinstein, B.M., Stemple, D.L., Driever, W., Fishman, M.C., 1995. Gridlock, a localized heritable vascular patterning defect in the zebrafish. *Nat. Med.* 1, 1143–1147.
- Westerfield, M., 1995. *The Zebrafish Book*. Univ. Oregon Press, Salem, Oregon.
- Zhong, T.P., Rosenberg, M., Mohideen, M.A., Weinstein, B., Fishman, M.C., 2000. gridlock, an HLH gene required for assembly of the aorta in zebrafish. *Science* 287, 1820–1824.
- Zhong, T.P., Childs, S., Leu, J.P., Fishman, M.C., 2001. Gridlock signalling pathway fashions the first embryonic artery. *Nature* 414, 216–220.